Scientific Journals
of the Maritime University of Szczecin

Zeszyty Naukowe
Akademii Morskiej w Szczecinie

2023, 75 (147), 20–34
ISSN 2392-0378 (Online)
DOI: 10.17402/570

Received: 29.04.2023
Accepted: 30.06.2023
Published: 30.09.2023

Assessment of sinkhole hazard in the post-mining area using the ERT method and numerical modeling

Roman Ścigała[1], Katarzyna Szafulera[2], Marek Jendryś[3]

[1] https://orcid.org/0000-0002-6927-091X
[2] https://orcid.org/0000-0001-7303-279X
[3] https://orcid.org/0000-0003-1159-1275

Silesian University of Technology, Faculty of Mining, Safety Engineering and Industrial Automation
2a Akademicka St., 44-100 Gliwice, Poland
e-mail: [1]roman.scigala@polsl.pl, [2]katarzyna.szafulera@polsl.pl, [3]marek.jendrys@polsl.pl
corresponding author

Keywords: shallow excavations, sinkhole threat, ERT method, numerical modeling, finite difference method, protection of mining areas

JEL Classification: Q4, Q5, Y8

Abstract

The loss of stability of shallow voids existing in the rock mass often results in the formation of sinkholes on the surface. This has a significant impact on the threat to public safety. Therefore, it is crucial to recognize the presence of such voids, especially in old post-mining areas, where shallow extraction was previously conducted, and there is a lack of mapping documentation indicating the location of underground workings. This paper presents an example illustrating a proposed procedure for recognizing shallow voids, which consists of two research works: geophysical research combined with numerical analyzes used as a kind of forward modeling. This combination increases the possibility of accurately locating potential sinkhole occurrences. The first part of this article provides selected literature information on the occurrence of sinkhole hazards. The second part presents the results of subsurface layer investigations of the rock mass conducted using electrical resistivity tomography (ERT). The third part focuses on assessing the threat of sinkhole formation by using forward numerical modeling performed with the FLAC 3D software to confirm the subsurface structures identified through the ERT method. The results of the analyzes conducted with both methods are then discussed in terms of their suitability for assessing the associated risk. The research conducted within the framework of this study confirms the effectiveness of the ERT method combined with numerical modeling for evaluating the state of the rock mass. This method can be considered a valuable tool for supporting decision-making in identifying post-mining areas that are particularly at risk of sinkhole formation.

Introduction

The loss of stability of shallow voids existing in the rock mass often results in the formation of sinkholes on the surface. This has a significant impact on the threat to public safety. Considering a large number of recent publications in the field of discontinuous deformations, especially sinkholes (Fu et al., 2021; Baluch et al., 2022; Dursun, 2022; Tufano et al., 2022; Vennari & Parise, 2022), it should be considered that this problem is relevant and current.

The creation of sinkholes on the ground surface is caused by both natural and human activity causes. The sinkholes may arise as a result of the occurrence of karst phenomena, as is well known in the USA state of Florida (Tihansky, 1999; Oliver-Cabrera et al., 2022). In such specific rock mass, the natural shallow caverns collapse, and sinkholes form on the surface. Similar cases are recorded in China (Zhou et

al., 2022), South Korea (Baluch et al., 2022), Turkey (Dursun, 2022), Italy (Vennari & Parise, 2022), and many other countries.

In Poland, discontinuous deformations of the surface type most often arise for anthropogenic reasons and usually are tied to mining activity (Chudek, Janusz & Zych, 1988; Fajklewicz et al., 2004; Pilecki, 2008; Kowalski, 2015; Strzałkowski, 2019, 2021). They mainly take the form of sinkholes ("cover-collapse" sinkholes), sometimes in the form of shallow subsidence troughs above the void without a visible break in the continuity of the surface – the so-called "cover-subsidence" sinkholes (Figure 1).

According to the majority of Polish researchers, shallow mining excavations located at depths of up to about 100 m (Chudek et al., 1988; Pilecki, 2008; Kowalski, 2015; Strzałkowski, 2019) pose a significant threat to the surface in the mining and post-mining areas. Many sinkholes are formed above the old shallow headings that are going to collapse. This is confirmed by the observations presented in previous works (Strzałkowski, 2021). This collapse is mainly due to the fact that these workings were not properly liquidated by filling – in fact, they are very often not liquidated at all after the cancellation of mine activity.

In Europe, sinkholes often occur in the areas of old, often already closed mines. An example may be sinkholes inventoried in France (Didier, 2009), Germany (Kretschmann, Efremenkov & Khoreshok, 2017), and Poland (Strzałkowski et al., 2021). The research carried out by Strzałkowski & Litwa (2020) showed that most cases of sinkholes occur in shallow mining excavations, which is related to the fact that the excavations occupy the largest area of the liquidated mine. In addition, threats are posed by headings and mining shafts driven in the 19th century and the beginning of the 20th century (Bell, 1988; Hunter, 2015; Strzałkowski et al., 2021). They pose a threat to the occurrence of sinkholes due to their improper liquidation in the past and shafts that were illegally driven, poorly secured, and not documented on mining maps.

To liquidate such a threat, an important issue is the precise localization of such shallow voids. Determining the location of the void can be carried out using a number of mining methods, including exploratory drilling, underground, and opencast mining works (excavations), as well as geophysical methods: GPR, gravimetric, seismic, or electrical resistivity (ERT) (Van Schoor, 2002; Cardarelli, Marrone & Orlando, 2003; Fajklewicz, 2007; Pringle et al., 2012; Łój, 2014; Madej, 2017; Łój & Porzucek, 2019). As mining methods are invasive ones and not always feasible, e.g., due to the existing surface development, therefore the geophysical methods (being non-destructive) have become increasingly important in recent years. An example of the use of this type of method to search for voids is studies conducted in Florida (Harro & Kiflu, 2018) or Brazil (Lago et al., 2022).

In the next Sections, we present an example illustrating a proposed procedure for recognizing the threat of sinkhole formation, which consists of two combined research works: geoelectrical investigation in search of shallow voids combined with numerical analyses used as a kind of forward modeling of their possible collapse due to loss of stability. The analyzes presented in this paper contribute to the recognition of the rock mass condition in post-mining areas. This recognition is crucial for minimizing construction hazards in new investments caused by possible sinkholes, and provides valuable data for selecting optimal protection works against such phenomena.

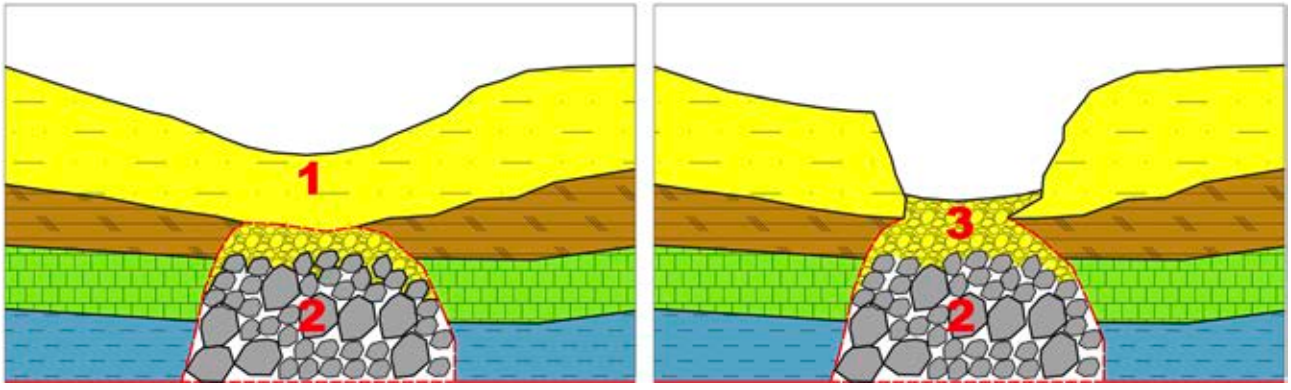

Figure 1. Cover – subsidence (left) and cover – collapse (right) sinkholes. Here, 1 is the micro-trough created over a shallow void (ground surface continuity is not broken), 2 is the shallow void of natural (e.g., karst) or anthropogenic origin (e.g., shallow mining working), and 3 is the collapsed part of the ground layers above the void (classical sinkhole)

Materials and methods

Description of the study area

The study area originates from one of the Polish coal mines located in the Upper Silesia Coal Basin (Figure 2). In this area, the shallow extraction of hard coal was conducted in the past (19th and 20th century) directly under the considered building plot (Figure 3). In 2010, a sinkhole was created near the north-east boundary of the building plot (Figure 3). It appeared above the old shallow heading located in coal seam 219, near the shallow shaft. The sinkhole diameter was about 3 meters, and its depth was about 2 m (Figure 4).

Figure 2. Location of the Upper Silesia Coal Basin over the Poland territory

Figure 4. Sinkhole created inside the area of the building plot over the old shallow mining workings

As mentioned earlier, a sinkhole occurred on the building plot near the garage building, affecting a section of the concrete slab pavement (Figure 4). To the west of the plot stands a detached residential building. In 2011, to assess the risk of further

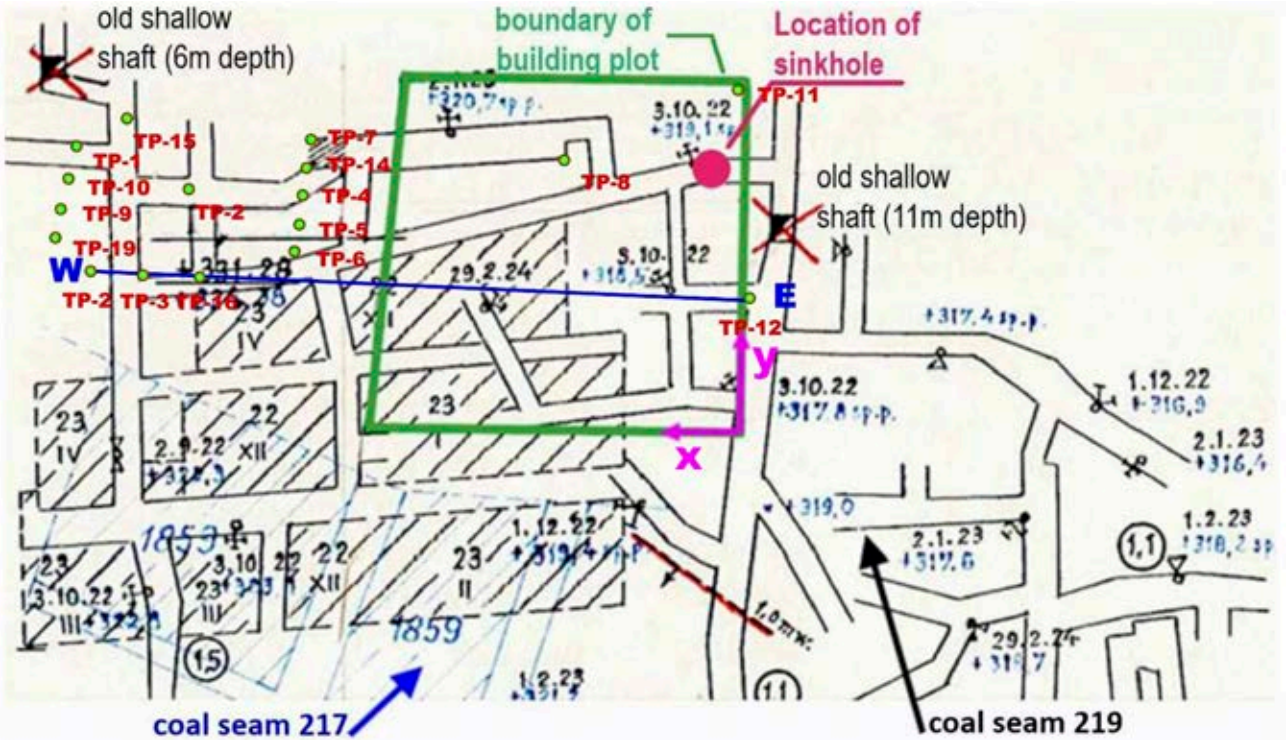

Figure 3. Map of the old shallow workings in coal seams 217 and 219 located in the study area (building plot boundary – green polygon) and location of the sinkhole created in 2010 (red dot), boreholes (green dots), and the course of geological cross-section W–E (blue line)

sinkholes and to protect the building from the impact of discontinuous deformations, drilling works were carried out, followed by treatment works. Seventeen boreholes were drilled, of which 14 were located in close proximity to each other (the area of the residential building), and the remaining 3 were scattered in the eastern part of the analyzed area (Figure 3) in the area of the sinkhole created in 2010. As a result of these works, no voids were found; in four boreholes, the presence of loosened zones was observed. The drilling works were not carried out over the entire area, but only on selected parts of the plot, which neighbored the residential building – west of the plot marked with a green polygon in Figure 3. Basic data on the exploration and technological boreholes drilled in the study area are presented in Table 1.

Table 1. Data on exploration and technological drilling in the study area

Borehole no.	Depth [m]	Thickness of overburden [m]	Data indicating the possible occurrence of old shallow workings along the borehole [running meters, RMT]
TP-1	15.0	4.0	–
TP-2	12.0	7.0	–
TP-3	11.0	7.5	–
TP-4	11.0	6.2	–
TP-5	13.3	6.3	6.30 RMT – 8.60 RMT: fractured coal
TP-6	11.0	6.5	–
TP-7	11.0	7.3	7.30 RMT – 8.30 RMT: loosened rock zone
TP-8	11.0	6.0	7.00 RMT – 7.80 RMT: loosened rock zone
TP-9	8.5	4.3	–
TP-10	8.0	4.2	4.20 RMT – 6.70 RMT: loosened rock zone
TP-11	11.3	5.1	–
TP-12	13.0	7.1	–
TP-13	8.5	6.0	–
TP-14	10.7	4.2	6.00 RMT – 8.00 RMT: clay mixed with coal
TP-15	8.2	5.1	5.10 RMT – 7.10 RMT: loosened rock zone
TP-16	10.0	7.1	7.10 RMT – 8.20 RMT: coal with pieces of wood
TP-17	8.6	5.3	–

Lithology and stratigraphy

The geological structure of the analyzed area was identified on the basis of 17 boreholes located on the building plot adjacent to the west boundary of the considered area (Figure 4). The boreholes were drilled due to the risk of sinkholes forming on the surface near the building being under construction. Lithological profiles of chosen boreholes in the area of the ERT survey are presented in Figure 5(a), and the geological cross-section drawn on their basis is illustrated in Figure 5(b). In stratigraphic terms, the geological structure of the near-surface part of the studied rock mass comprises Quaternary and Carboniferous formations.

Overburden Quaternary layers are present in the whole area of the plot, represented mainly by sands and clays, and their thickness ranges from 4.0 m to 7.5 m (Table 1). The Carboniferous formations are represented by the "Łaziskie" strata – group "200" (named according to the Polish classification of Carboniferous layers). Up to the depth of exploration (about 15 m), they are mainly developed in the form of shales and hard coal layers. The Carboniferous strata dip to the south-east at an angle not exceeding 3°. No tectonic faults or other disturbances inside the rock mass were found in the study area.

Mining operations carried out in the vicinity of the study area

Mining in the study area was carried out in two coal seams. In 1859, seam 216 was mined, while between 1922 and 1924, seam 219 was extracted. Exploitation was carried out at depths of between approximately 9 m and approximately 11 m, using a longwall system with roof caving. The thickness of the extracted seams was about 1.5 m. A sketch illustrating the mining situation is presented in Figure 3. It can be seen that in the rock mass in the study area, there are mainly horizontal galleries and goafs in seam 219. Mining workings in seam 217 are found only in the south-western part of the studied area. The location of the old shafts is related to the accessing of seam 219, with depths of up to 6 m and 11 m. Figure 3 also shows, marked with a purple color, the local coordinate system (X, Y), which was used as a reference element in further drawings presented in this paper.

The description of deformations created on the surface

The occurrence of non-liquidated or partly liquidated mine workings and the presence of numerous loosened zones in the rock mass (Table 1) pose a high risk of the formation of discontinuous deformations, mainly of sinkhole type. In the area of the conducted

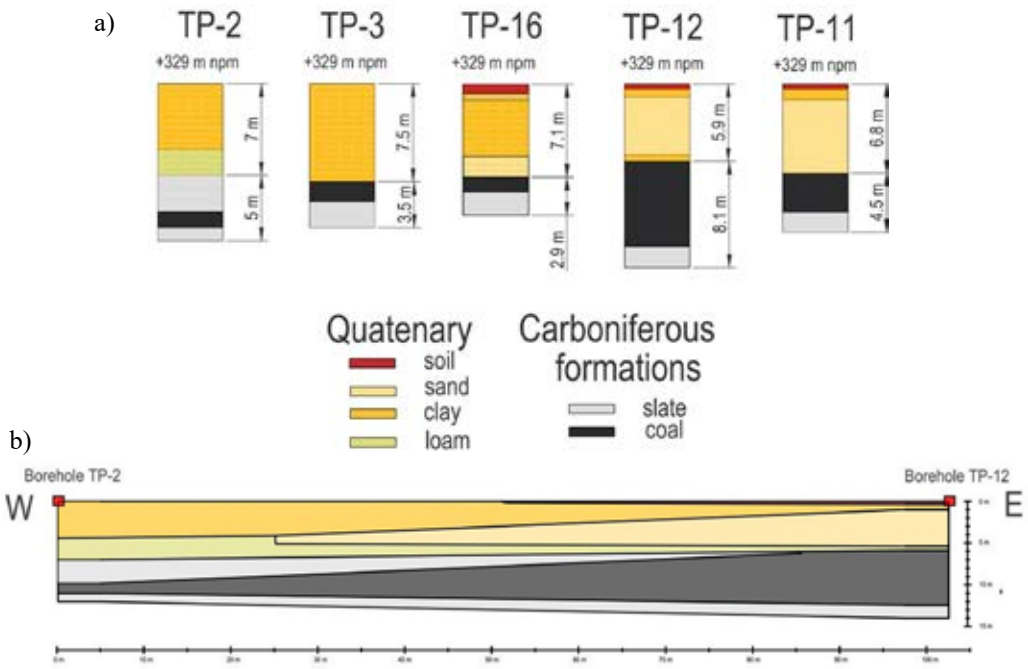

Figure 5. Geological structure of the near-surface layers in the study area (a) lithological profile of borehole: TP-2, TP-3, TP-16, TP-12, and TP-11 – (area of ERT sounding) and (b) geological cross-section W-E

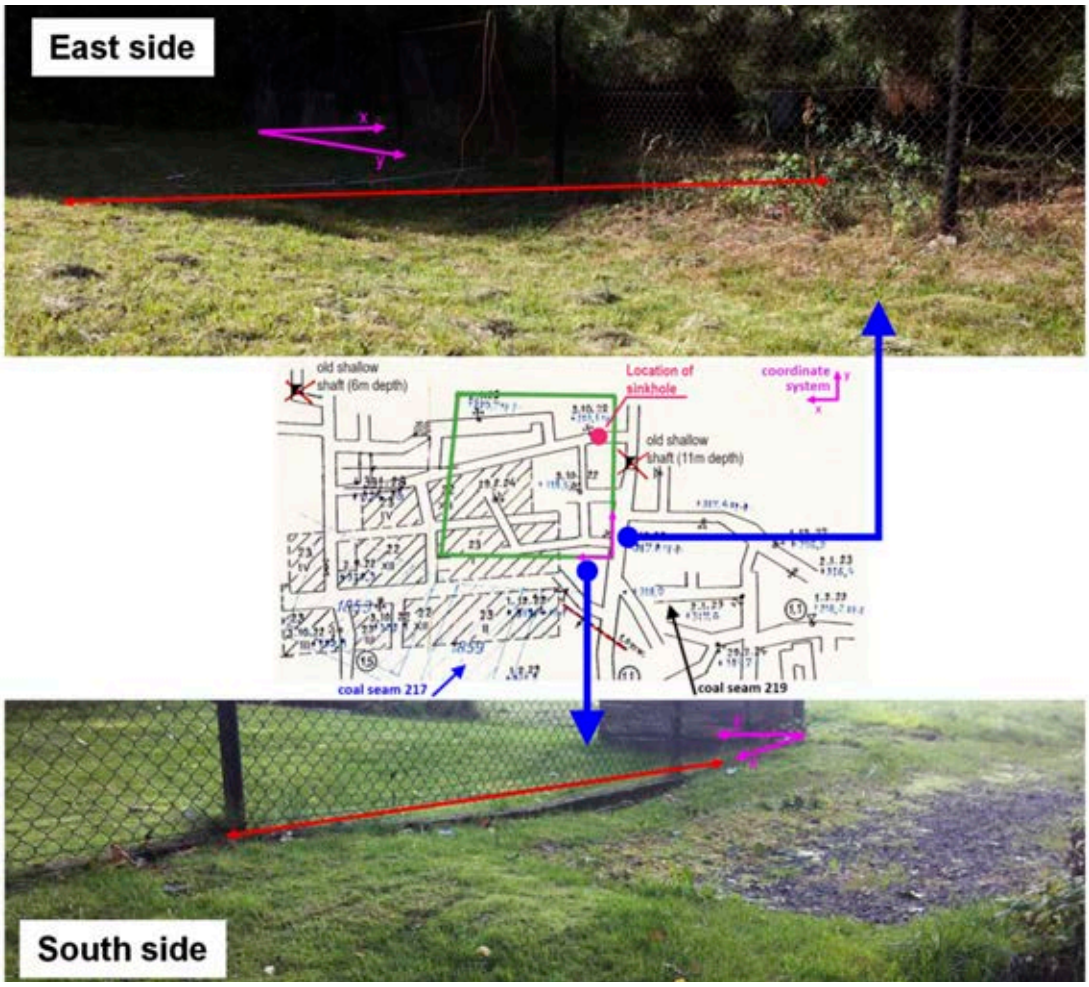

Figure 6. Deformations observed on the surface: micro-subsidence troughs (cover-subsidence sinkholes) near the border of the plot

research, apart from the sinkhole formed in 2010 (Figures 3 and 4), "pseudo-continuous deformations" are currently being created in the southern and eastern boundaries of the plot (Figure 6). They take the form of "cover-subsidence" sinkholes, resembling shallow basins (or micro-subsidence troughs) with a diameter of approximately several meters.

The location of these deformations can be associated with the existence of shallow excavations in seam 219 (Figure 3), which presumably have not been properly filled. The workings date back to the beginning of the 19th century; hence, there is no information on whether they were properly liquidated.

Conducted ERT survey

For the purpose of assessing the structure of shallow rock mass layers in the area of micro-subsidence troughs occurrence on the surface in question, ERT investigations were performed. The Ares II equipment made by Czech company GF-Instruments was used for the tests (GF Instruments, 2021). The profile designed for the ERT investigations consisted of 48 electrodes arranged along a straight line at 1.5 m intervals. The total length of the profile was 70.5 m. In light of the literature and practical experiences (Loke MH & Barker RD 1996; Loke, 2013; GF Instruments, 2021), the maximum depth of penetration with such a line length and Wenner/Schlumberger arrays used is approximately 1/5 of the line length, which in the presented case corresponds to a depth of about 13 m. The survey line was located latitudinally along the south boundary of the building plot in such a way that it passed through the southern micro-trough (Figure 6) over the "X" direction of the local coordinate system (Figure 7). Two measuring arrays were used in the ERT sounding: "Wenner α" and "Wenner-Schlumberger" (Loke & Barker, 1996; Fajklewicz, 2007; Loke, 2013; GF Instruments, 2021). The configuration of the ERT survey line is presented in Figure 7, along with two photographs from the west and east end of the line.

For processing the ERT results, the software RES-2DINV (Loke, 2013) was used. The distribution of resistivity over the analyzed cross-section obtained with the Wenner-Schlumberger array is presented in Figure 8. The discussion of the results is given in the next Section.

Figure 7. View of the ERT survey line

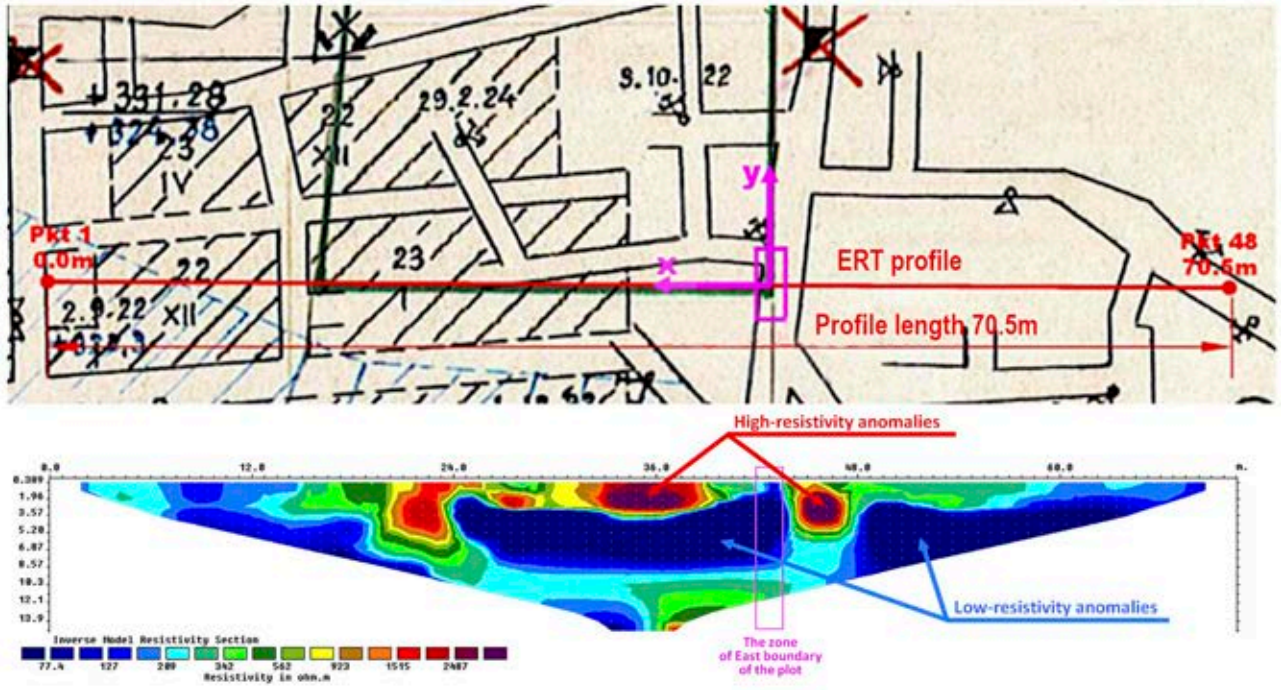

Figure 8. Distribution of the shallow subsurface layers' resistivity obtained for the WennerSchlumberger array

Numerical modeling procedure

Assumptions to numerical investigation

To analyze the safety of surface facilities and the possibility of deformation of the ground surface due to the loss of stability of old shallow mine workings, an attempt was made to represent such a situation by means of numerical modeling. The region of the considered building plot, characterized in a previous Section, was analyzed. As described above, in the analyzed region, very shallow coal seams were extracted. As a result of this exploitation, a number of drifts located at shallow depths remained, usually with timber support, and not filled after their closure.

To recognize the approximate state of the rock mass in the study area, a number of numerical simulations were carried out using software based on the finite difference method: Itasca FLAC. The Itasca FLAC (Itasca Consulting Group, 2009) allows for two- and three-dimensional modeling of the behavior of ground, rock, and other media, both in elastic terms and considering the plastic flow of the material after a critical state is reached. In the software used, the medium (rock mass) being modeled is represented by polyhedral elements divided into a spatial grid of finite difference elements so that the user can match the geometry of the model to the real object. Each element, as a result of an applied force or displacement boundary conditions, behaves according to its assigned mechanical constitutive model, which defines the stress-strain relationship. During the simulations, plasticization and flow of the material can occur, and the finite difference elements may deform and move with the modeled object.

The computational scheme used allows for the modeling of material failure and its post-critical states. The program does not require the construction and solving of stiffness matrices (in contrast to FEM-based software), which makes it possible to build very complex models with relatively low hardware requirements. The applicability of this software for modeling underground mining workings (Prusek & Bock, 2008; Guo et al., 2019; Kong et al., 2019), as well as tunnels (Monjezi et al., 2012; Hassanlourad, Naghizadehrokni & Molaei, 2019; Hu & Wang, 2019), is confirmed by numerous publications.

Simulations were carried out for three variants of a 2D model representing the rock mass in a vertical section through a shallow gallery, and for a 3D model that considers the mining–geological conditions and the layout of the excavations in the analyzed area (Figure 9). The simulations were performed for an elastic-plastic model with weakening, using the Coulomb-Mohr strength condition described by:

$$f^s = \sigma_1 - \sigma_3 N_\phi + 2c\sqrt{N_\phi} \tag{1}$$

and the limitation of tensile stress transfer to tensile strength according to the relationship:

$$f_t = \sigma_3 - \sigma^t \tag{2}$$

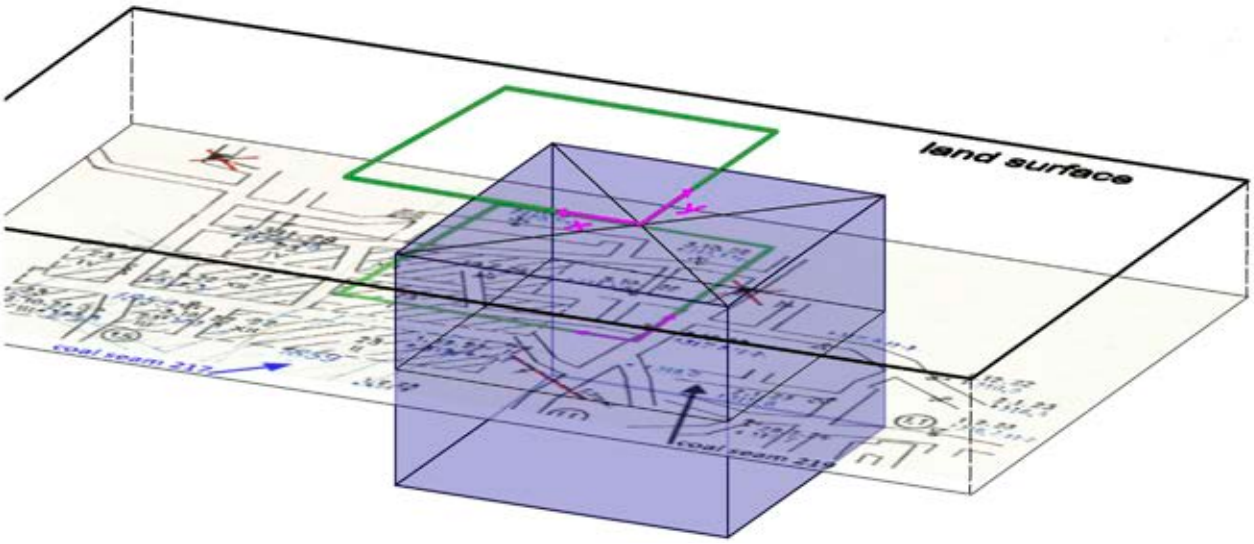

Figure 9. Location of the 3D numerical model in relation to the considered building plot on the land surface

Here, σ_1 represents the highest principal stress, σ_3 is the lowest principal stress, and c is the cohesion. Moreover,

$$N_\phi = \frac{1+\sin\varphi}{1-\sin\varphi} = \tan^2\left(45+\frac{\varphi}{2}\right),$$

in which φ is the angle of internal friction.

Simulations of rock mass conditions in the vicinity of the analyzed voids

The state of the rock mass in the vicinity of the voids in question was analyzed using numerical models, the geometry of which is shown in Figure 10. In the model layers, different material properties have been used (summarized in Table 2).

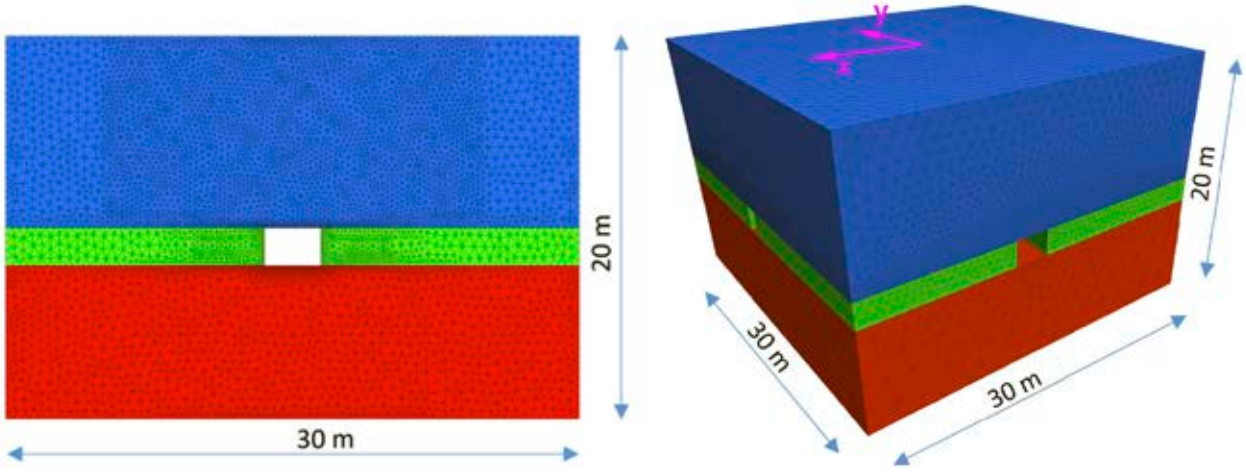

Figure 10. Geometry of the analyzed numerical models

Table 2. Material parameters used in the numerical model

No.	Material	Depth H [m]	Cohesion c [kPa]	Angle of internal friction φ [deg]	Tension limit Rt [kPa]	Bulk modulus K [MPa]	Shear modulus G [MPa]	Density r [kg/m^3]
1	Quaternary layers	0–10	10	30	0	109	50	2100
2	Coal bed	10–12	500	25	100	1500	1000	1500
3	Carboniferous layers	12–20	750	30	100	3000	2000	2300
4	Filling	10–11.9	5	35	0	111	37	2100

To investigate the possibility of surface deformation creation in the considered area, simulations were carried out on 2D models with structural elements representing the timber support casings that protect the excavation during its construction and use (such support was used for the protection of the workings in this area in the 19th century, when they were constructed). The timber support was modeled by introducing two-dimensional bar elements on the contours of the excavated heading (Figure 11). The following properties were used for the bar elements simulating the support:

- cross-sectional area: $A = 0.031$ m^2,
- moment of inertia: $I = 0.0019$ m^4,
- Young modulus: $E = 10$ GPa,
- Poisson ratio: $v = 0.3$.

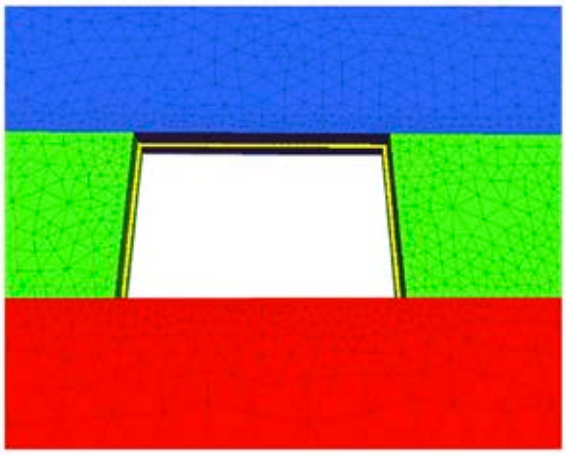

Figure 11. Location of the bar elements simulating timber support

As a result of the large deformations caused by the plastic flow of the material to be modeled, the roof of the gallery subsides to the floor. To prevent, in the numerical simulations, the upper edge of the excavation from overlapping with the lower one, and to model the contact between the roof and floor or the roof and backfill, the contact elements of the "interface" type (in FLAC's nomenclature) were used in the roof of the excavation (Figure 12).

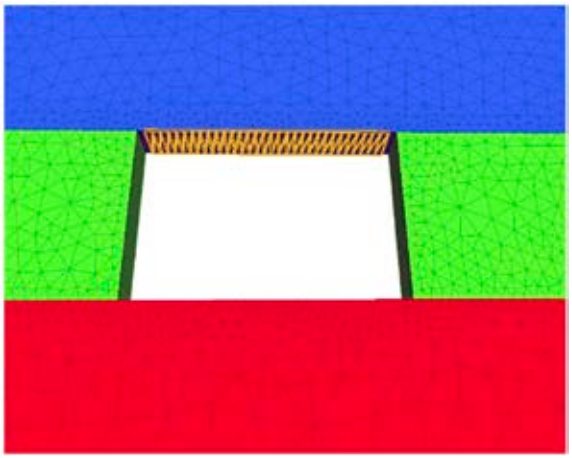

Figure 12. Location of the contact elements of the "interface" type

Simulations using the 2D model were carried out for three variants:

- A model reproducing the state of the rock mass in the vicinity of an excavation protected by support.
- A model simulating the rock mass in the case of support destruction (in FLAC's procedure, the removal of elements simulating the support is completed); the model assumes that in the long run, as a result of unfavorable environmental conditions, the timber support is being degraded. This leads to a decrease in its bearing capacity resulting in its total destruction. Such a situation for an exemplary excavation is presented in Figure 13.

Figure 13. Collapses in the underground gallery caused by damage occurred to the timber support

- A model representing the state of the rock mass in the case of backfilling of the abandoned gallery with simultaneous degradation of its support.

Discussion of results

Results of the ERT surveys

As was stated earlier, the ERT investigations were conducted with two arrays: Wenner α and Wenner-Schlumberger. Due to the limited length of this paper, only the results obtained with the Wenner-Schlumberger array are presented in Figure 8. Analyzing the distribution of resistivity over the vertical cross-section along the length of the measurement line, several characteristic structures with clearly distinguished resistivity can be observed:

- The most distinctive oval-shaped anomaly is visible to the east of the eastern boundary of the building plot. This anomaly shows high resistivity values relative to the surrounding area (approximately 2500 Ωm) and has a very distinctive cross-sectional shape, suggesting the presence of a secondary void at this location, most likely related to the presence of a not liquidated mining gallery. A similar zone of high resistivity occurs on the western side of this boundary. This corresponds with the situation on the mine workings map shown in Figure 13, where mine workings (i.e., galleries) are visible running along the eastern and southern boundaries of the plot.
- Below the shallow rock mass structures of relatively high resistivity, extensive structures of considerably lower resistivity (about 100 Ωm) are visible, which can be identified with old post-mining goafs that can accumulate water infiltrating from the surface.

Results of the numerical modeling

The results of the simulation made with the FLAC software, recovering the probable rock mass state in the surroundings of the excavation protected by the timber support, are presented by means of the distribution of plastic zones and the distribution of vertical displacements shown in Figures 14 and 15.

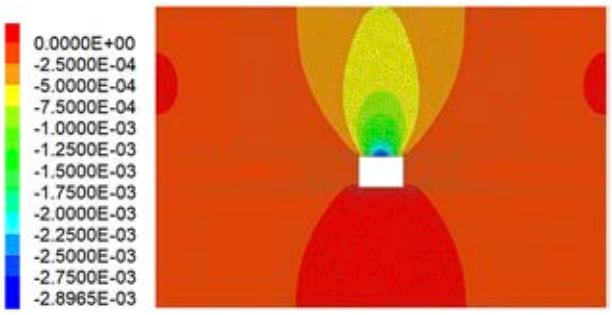

Figure 15. Vertical displacements (subsidence) in the model with support–protected excavation

In the results presented below, the plastic zones resulting from the reaching of the tensile strength – denoted as "tension" in the legend – and the shear strength by satisfying the Coulomb strength condition – denoted as "shear" – are marked separately by means of differentiated colors. Due to the iterative calculation method, the results can also distinguish whether the limit state is reached in the current calculation step ("shear-n" and "tension-n") or was reached in earlier iterations ("shear-p" and "tension-p"). Elements where the stress state has not reached the limit value are marked with a gray color ("none").

As shown in the figures below, the excavation with support is stable with relatively small zones of plasticization in its vicinity, extending into the rock mass at a distance of 1.8 m (Figure 14) and maximum

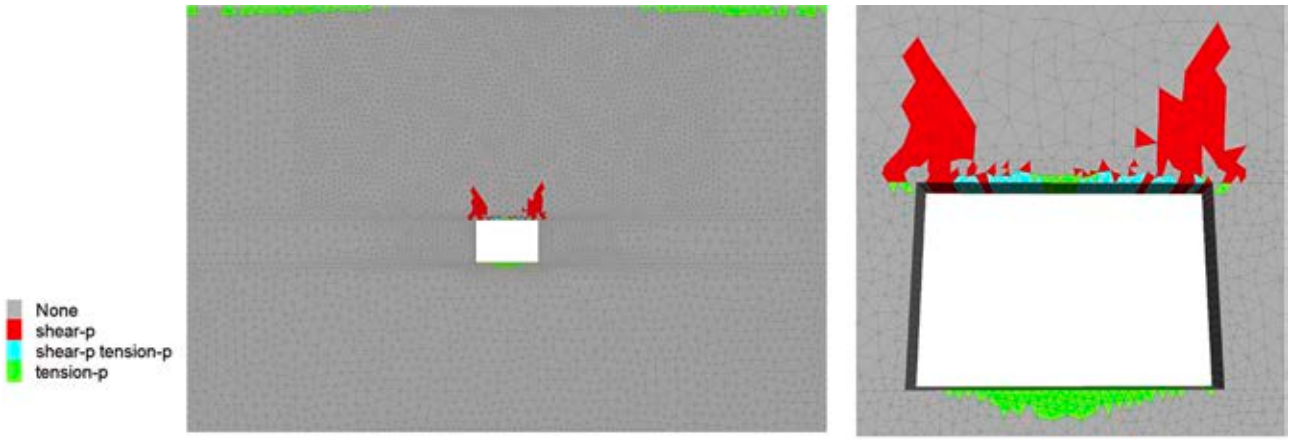

Figure 14. Plastic zones in the model with support–protected excavation (gallery)

vertical displacements in the roof of the excavation reaching nearly 3 mm (Figure 15).

The results of the simulations for variant II are presented in Figures 16 and 17. In this variant, a situation was reproduced in which a failure of the support occurred, resulting in the formation of extensive failure zones extending from the roof of the gallery to the ground surface. The plasticized material moved towards the excavation, finally filling it completely (Figure 17) and causing surface deformations characterized by subsidence exceeding 0.5 m.

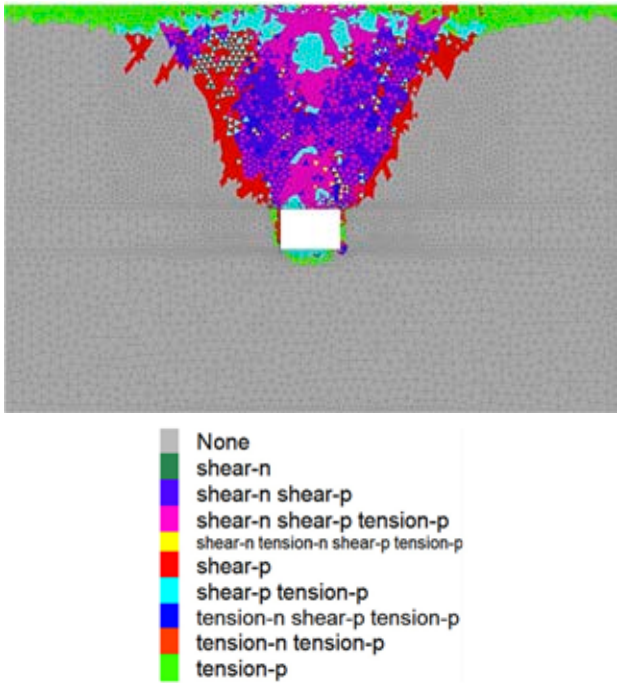

Figure 16. Plastic zones in the model with excavation without support

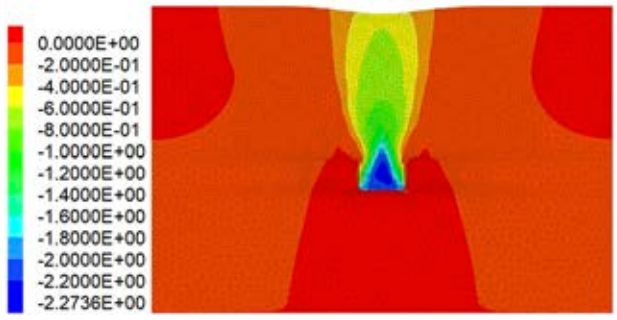

Figure 17. Vertical displacements (subsidence) in the model with excavation without support

The occurrence of old shallow workings in the investment areas poses a significant threat to the surface facilities constructed in their vicinity. One method of counteracting such a hazard is to eliminate voids in the rock mass by backfilling them, which has been tested in variant III of the numerical simulations. In this variant, it is assumed that the excavation is filled with backfill material to a height of 1.9 m and that the timber support has been destroyed. In this case, a limit state of stress is reached between the roof of the excavation and the land surface, resulting in the plasticization of the material, as shown in Figure 18. However, in this case, the deformation of the rock mass is significantly reduced, with maximum surface subsidence not exceeding 34 mm (Figure 19).

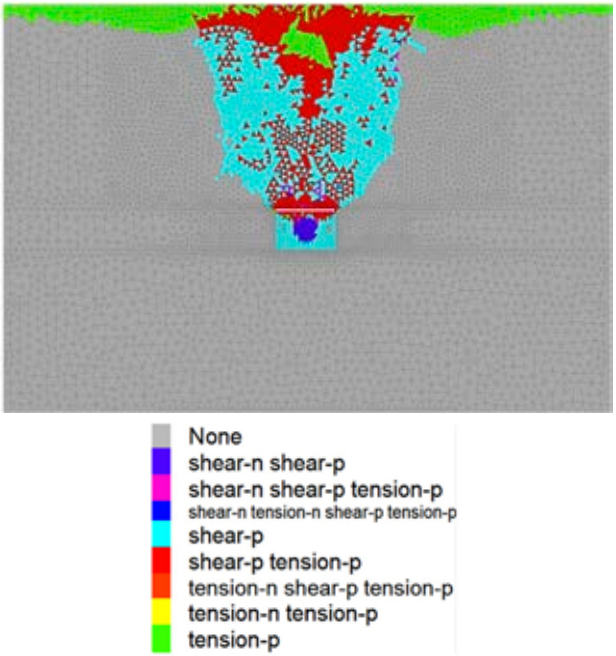

Figure 18. Plastic zones in the model with excavation liquidated by backfilling

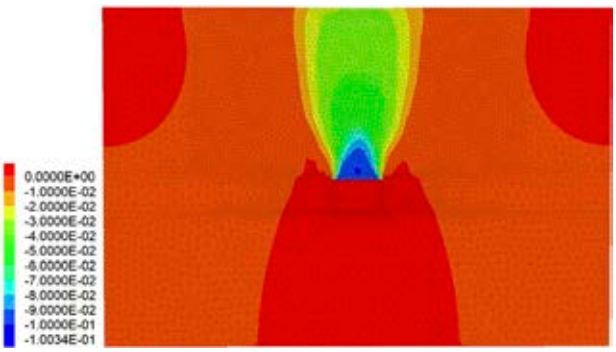

Figure 19. Vertical displacements in the model with excavation liquidated by backfilling

Due to the extensive spatial arrangement of the workings in the area under consideration, a simulation was also carried out for a model comprising a three-dimensional rock mass volume (Figure 20). In this model, workings were reproduced from the map of seam 219, with the simulation carried out for the most unfavorable variant assuming the destruction

of the excavations and, as a consequence, a lack of support in the galleries.

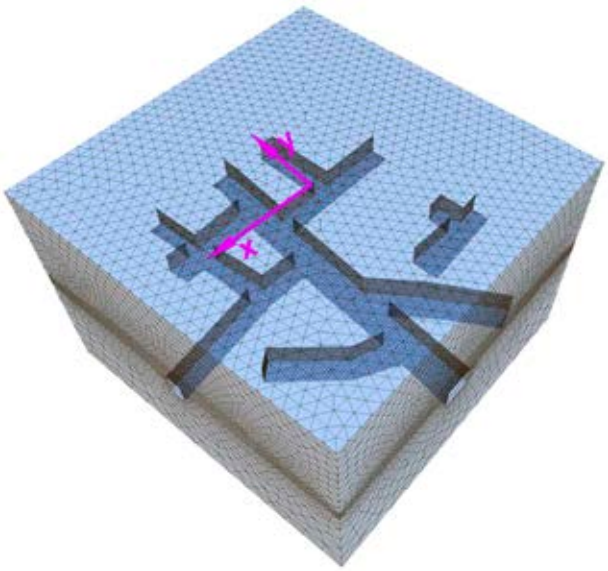

Figure 20. 3D numerical model of the rock mass with the location of main galleries in coal seam 219

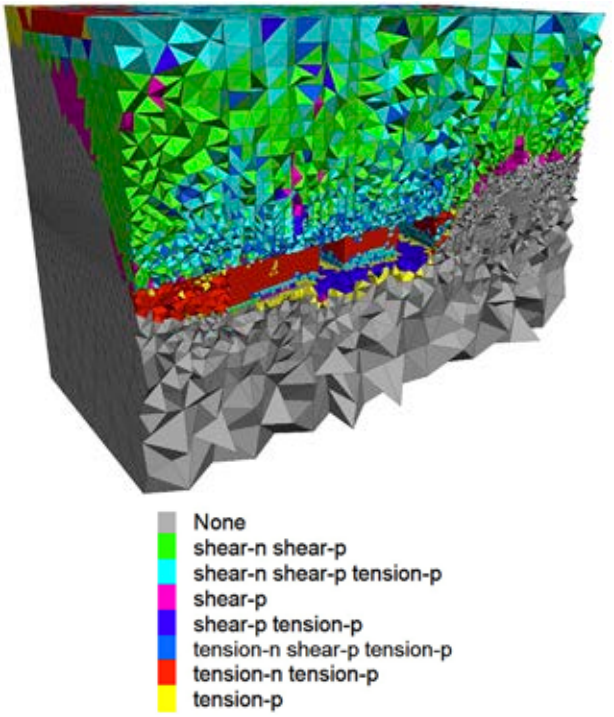

Figure 21. Plastic zones in the 3D model, vertical cross-section

The results obtained are presented in the same way as for the 2D models, i.e., in the form of plastic zone and vertical displacement distributions. The zones of plasticization are shown in the vertical cross-section (Figure 21), crossing the central part of the model in the east-west direction. This indicates that, in the case of failure of the support and rockfall into the workings, the zones of failure manifested by plasticization of the material reach the ground surface. This process leads to the creation of a secondary equilibrium state and a change in the original mechanical and filtration parameters of the soils present in the area, which may have consequences for the designed structures on the surface.

The maximum vertical displacement was experienced by the elements forming the roof of the workings, with the displacement reaching 2 m (Figure 22), which corresponds to the height of the modeled workings. With the distance from the roof of the workings, the values of the vertical displacements decrease, reaching a value close to 0.4 m at the surface. As shown in Figure 23, the deformation of

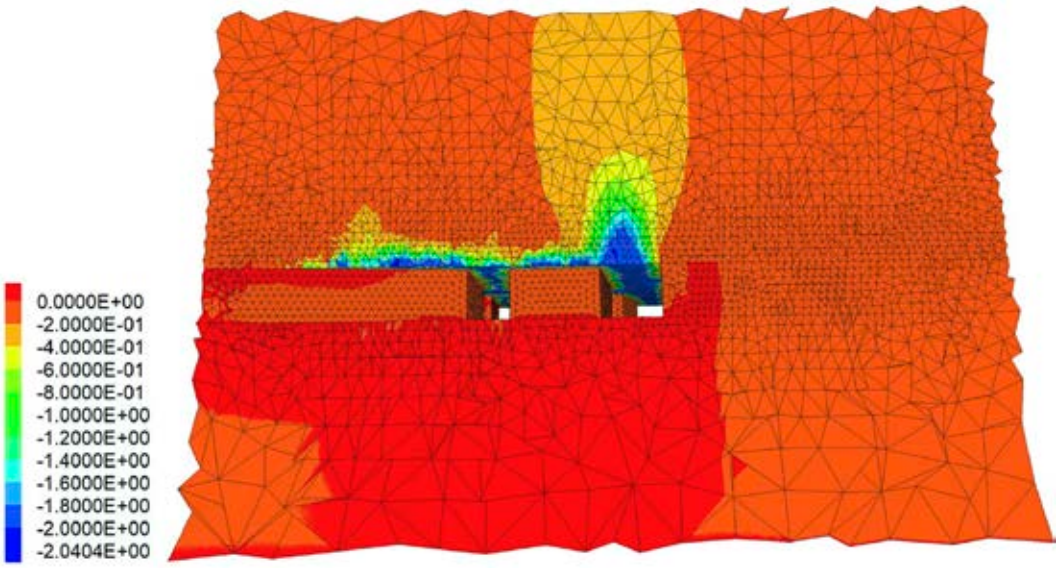

Figure 22. Vertical displacements in the 3D model along the vertical cross-section

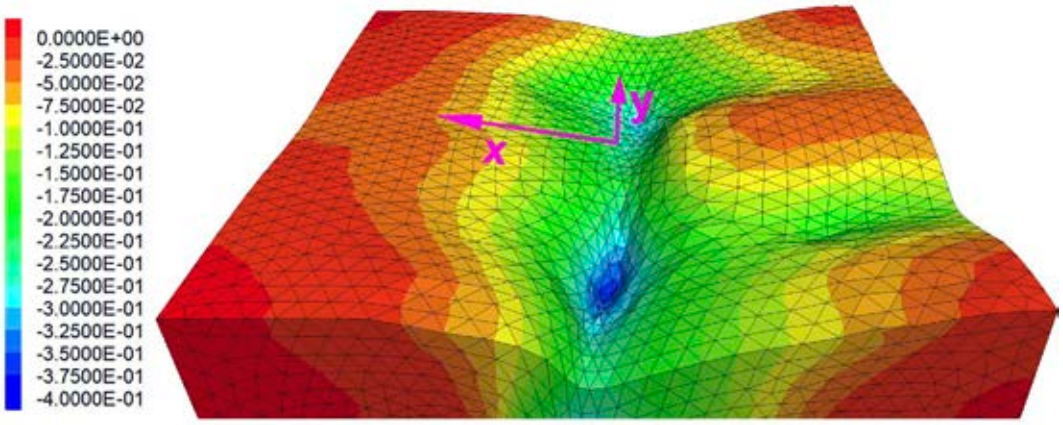

Figure. 23. Vertical displacements (subsidence) of the modeled ground surface (deformations magnified ×15)

the surface depends on the layout of the workings, with maximum subsidence occurring in the areas of crossings of galleries.

When comparing the results of the modeling with the actual state, it should be borne in mind that the model represents the final state in which roof collapse has occurred along the entire length of the modeled workings. In reality, this process does not occur simultaneously in all the workings, and the local roof collapses and accompanying surface subsidence may occur at varying and difficult to predict moments.

Conclusions

In this paper, the results of analyses carried out to assess the surface hazard for the possibility of arising sinkhole-type discontinuous deformation have been presented. Investigations were carried out by means of shallow rock mass penetration using electrical resistivity tomography (ERT), followed by analyzes of the stress state of the rock mass in the area between old shallow mine workings and the ground surface using numerical modeling. Numerical simulations were carried out with FLAC 3D software, which is based on the finite difference method. The research was conducted in the mining area of one of the Upper Silesia Basin coal mines, where shallow underground mining was carried out in the past – in the 19th and early 20th centuries. To summarize the research carried out, the following concluding remarks can be stated:

1. In typical geological conditions of sedimentary deposits, including the Polish Upper Silesian Coal Basin, a sinkhole hazard is to be expected if unprotected voids of both natural and anthropogenic origin are present at depths of up to about 100 meters.
2. In the case of anthropogenic voids, we are most often dealing with the post-mining workings of old, usually closed mines. It should be noted that while the threat from continuous deformations (subsidence troughs) occurs at most a few years after the end of underground mining works (usually several months) and then decays, in the case of shallow, not liquidated (backfilled) workings, the sinkhole threat will occur on the surface for a very long time – even several decades after the end of mining activities. In fact, it should be stated that, due to the processes of support destruction over time, the sinkhole threat level will usually increase.
3. A number of methods can be used to assess the hazard level (especially to identify where shallow voids exist); the most precise are mining methods in the form of drilling or opencast investigations. However, these methods are highly intrusive to the environment, both natural and urbanized, and are time- and capital-consuming. An alternative is the use of geophysical methods, which make it possible to assess the approximate structure of the near-surface rock mass layers in a non-destructive manner. However, it should be borne in mind that they do not provide 100% certainty of the location of underground voids.
4. The optimum configuration in terms of identifying this type of hazard is to use geophysical methods over a wider area to select zones where anomalies have been found, which allows the assumption that voids exist in such places. Boreholes should then be drilled in such areas to confirm the presence of voids, which can then be eliminated by filling them with suitable material and, thus, eliminating the sinkhole hazard.
5. Research carried out within the framework of this study confirms the effectiveness of the ERT

method in the scope indicated above. It should also be noted that the numerical modeling of the rock mass state, which was additionally used in this study, effectively complements the analysis of sinkhole hazards. This may be considered as an excellent tool for supporting decision-making in the field of identification of areas particularly endangered and drilling in such places in order to confirm the occurrence of shallow voids (enabling their later elimination). Supplemented in this way, the procedure makes possible more efficient minimization of the costs of reclamation of post-mining areas at risk of sinkholes.

References

1. Baluch, K., Kim, J.-G., Kim, J.-G., Ko, Y.-H., Jung, S.-W. & Baluch, S.Q. (2022) Assessment of sinkholes investigations in Jangseong-Gun area, South Korea, and recommendations for similar studies. *International Journal of Environmental Research and Public Health* 19(3), 1111, doi: 10.3390/ijerph19031111.
2. Bell, F.G. (1988) Land development. State of the art in the location of old mine shafts. *Bulletin of the International Association of Engineering Geology* 37, pp. 91–98, doi: 10.1007/BF02590374.
3. Cardarelli, E., Marrone, C. & Orlando, L. (2003) Evaluation of tunnel stability using integrated geophysical methods. *Journal of Applied Geophysics* 52(2), pp. 93–102, doi: 10.1016/S0926-9851(02)00242-2.
4. Chudek, M., Janusz, W. & Zych, J. (1988) *Study on diagnosis and prognosis of the formation of discontinuous deformation due to underground mining*. Scientific Journal of Silesian University of Technology, Gliwice, vol. 141, no. 165 (in Polish).
5. Didier, C. (2009) Postmining management in France: situation and perspectives. *Risk Analysis* 29(10), pp. 1347–1354, doi: 10.1111/j.1539-6924.2009.01258.x.
6. Dursun, A.E. (2022) Risk analysis of natural sinkholes hazards in Karapınar basin (Konya, Turkey). *Arabian Journal of Geosciences* 15(3), 279, doi: 10.1007/s12517-022-09564-8.
7. Fajklewicz, Z. (2007) *Applied Gravimetry*. Kraków: AGH University of Science and Technology Press.
8. Fajklewicz, Z., Piwowarski, W., Radomiński, J., Stawarski, E. & Tajduś, A. (2004) Badanie deformacji w górotworze w celu odtwarzania wartości budowlanej terenów pogórniczych. Kraków: Wyd. AGH (In Polish).
9. Fu, Y., Shang, J., Hu, Z., Li, P., Yang, K., Chen, C., Guo, J. & Yuan, D. (2021) Ground fracture development and surface fracture evolution in N00 method shallowly buried thick coal seam mining in an arid windy and sandy area: A case study of the Ningtiaota mine (China). *Energies* 14(22), 7712, doi: 10.3390/en14227712.
10. GF Instruments (2021) *ARES II – Automatic Resistivity and IP System, Brno, Czech Republic*. [Online]. Available from: http://www.gfinstruments.cz [Accessed: March 30, 2021].
11. Guo, Z.M., Zhang, L., Ma, Z., Zhong, F., Yu, J. & Wang, S. (2019) Numerical investigation of the influence of roof fracturing angle on the stability of gob-side entry subjected to dynamic loading. *Shock and Vibration* 2019, 1434135, doi: 10.1155/2019/1434135.
12. Harro, D. & Kiflu, H. (2018) *Imaging of Deep Sinkholes Using the Multi-electrode Resistivity Implant Technique (MERIT) Case Studies in Florida*. National Cave and Karst Research Institute Symposium 7, pp. 341–345, doi: 10.5038/9780991000982.1026.
13. Hassanlourad, M., Naghizadehrokni, M. & Molaei, V.A. (2019) A numerical study of seismic response of shallow square tunnels in two-layered ground. *International Journal of Geological and Environmental Engineering* 13(3), pp. 167–174.
14. Hu, B. & Wang, Ch. (2019) Ground surface settlement analysis of shield tunneling under spatial variability of multiple geotechnical parameters. *Heliyon* 6(9), e02495, doi: 10.1016/j.heliyon.2019.e02495.
15. Hunter, J. (2015) Old mines and new sinkholes along the Hucklow Edge vein, Derbyshire. *Mercian Geologist* 18(4), pp. 213–226.
16. Itasca Consulting Group (2009) *FLAC 3D User's Guide*. Minneapolis.
17. Kong, P., Jiang, L., Jiang, J., Wu, Y., Chen, L. & Ning, J. (2019) Numerical analysis of roadway rock-burst hazard under superposed dynamic and static loads. *Energies* 12(19), 3761, doi: 10.3390/en12193761.
18. Kowalski, A. (2015) *Deformacje powierzchni w Górnośląskim Zagłębiu Węglowym*. Katowice: Główny Instytut Górnictwa.
19. Kretschmann, J., Efremenkov, A. & Khoreshok, A. (2017) From mining to post-mining: the sustainable development strategy of the German hard coal mining industry. *IOP Conference Series: Earth and Environmental Science* 50, 012024. doi: 10.1088/1755-1315/50/1/012024.
20. Lago, A.L., Borges, W.R., Barros, J.S. & de Sousa Amaral, E. (2022) GPR application for the characterization of sinkholes in Teresina, Brazil. *Environmental Earth Sciences* 81, 132, doi: 10.1007/s12665-022-10265-4.
21. Loke, M.H. & Barker, R.D. (1996) Practical techniques for 3D resistivity surveys and data inversion. Geophysical Prospecting 44(3), pp. 499–523, doi: 10.1111/j.1365-2478.1996.tb00162.x.
22. Loke, M.H. (2013) RES2DINV – Geoelectrical Imaging 2D & 3D, a practical guide to 2-D and 3-D surveys. Malaysia 1997–2000. Geotomo software, Malaysia.
23. Łój, M. (2014) Microgravity monitoring discontinuous terrain deformation in a selected area of shallow coal extraction. In *Proceedings of the 14th International Multidisciplinary Scientific GeoConference SGEM*, Albena, Bulgary, Vol. 1, pp. 521–528.
24. Łój, M. & Porzucek, S. (2019) Detailed analysis of the gravitational effects caused by the buildings in microgravity survey. *Acta Geophysica* 67, pp. 1799–1807, doi: 10.1007/s11600-019-00336-9.
25. Madej, J. (2017) Gravity surveys for assessing rock mass condition around a mine shaft. *Acta Geophysica* 65, pp. 465–479, doi: 10.1007/s11600-017-0043-8.
26. Monjezi, M., Babak, N.F., Seyed, R.T. & Trilok, N.S. (2012) Stability analysis of a shallow depth metro tunnel: a numerical approach. *Archives of Mining Sciences* 57(3), pp. 535–545, doi: 10.2478/v10267-012-0035-0.
27. Oliver-Cabrera, T., Wdowinski, S., Kruse, S. & Robinson, T. (2022) Detection of sinkhole activity in West-Central Florida using InSAR time series observations. *Remote Sensing of Environment* 269, 112793, doi: 10.1016/j.rse.2021.112793.

28. Pilecki, Z. (2008) The role of geophysical methods in the estimation of sinkhole threat in the post-mining areas of shallow exploitation in the Upper Silesian Coal Basin, Poland. *Mineral Resources Management* 24(3/1), pp. 27–40.
29. Pringle, J.K., Styles, P., Howell, C.P., Branston, M.W., Furner, R. & Toon, S.M. (2012) Long-term time-lapse microgravity and geotechnical monitoring of relict salt mines, Marston, Cheshire, UK. *Geophysics* 77(6), pp. 287–294, doi: 10.1190/geo2011-0491.1.
30. Prusek, S. & Bock, S. (2008) Assessment of rock mass stresses and deformations around mine workings based on three-dimensional numerical modeling. *Archives of Mining Sciences* 53(3), pp. 349–360.
31. Strzałkowski, P. (2019) Sinkhole formation hazard assessment. *Environmental Earth Sciences* 78(1), 9, doi: 10.1007/s12665-018-8002-5.
32. Strzałkowski, P. (2021) The influence of selected mining and natural factors on the sinkhole creation hazard based on the case study. *Environmental Earth Sciences* 80, 117, doi: 10.1007/s12665-021-09403-1.
33. Strzałkowski, P. & Litwa, P. (2020) Environmental protection problems in the areas of former mines with emphasis on sinkholes: selected examples. *International Journal of Environmental Science and Technology* 18, pp. 771–780, doi: 10.1007/s13762-020-02860-4.
34. Strzałkowski, P., Ścigała, R., Szafulera, K. & Kołodziej, K. (2021) Surface deformations resulting from abandoned mining excavations. *Energies* 14(9), 2495, doi: 10.3390/en14092495.
35. Tihansky, A.B. (1999) Sinkholes West-Central Florida. A link between surface water and ground water. In: Galloway, D.L., Jones, D.R., Ingebrtsen, S.E. *Land Subsidence in the United States*. U.S. Geological Survey, Circular 1182, pp. 121–140.
36. Tufano, R., Guerriero, L., Annibali Corona, M., Bausilio, G., Di Martire, D., Nisio, S. & Calcaterra, D. (2022) Anthropogenic sinkholes of the city of Naples, Italy: an update. *Natural Hazards* 112, pp. 2577–2608, doi: 10.1007/s11069-022-05279-x.
37. Van Schoor, M. (2002) Detection of sinkholes using 2D electrical receptivity imaging. *Journal of Applied Geophysics* 50(4), pp. 393–399, doi: 10.1016/S0926-9851(02)00166-0.
38. Vennari, C. & Parise, M.A. (2022) Chronological database about natural and anthropogenic sinkholes in Italy. *Geosciences* 12(5), 200, doi: 10.3390/geosciences12050200.
39. Zhou, Y., Zhao, L., Cao, J. & Wang, Y. (2022) Using an improved SWAT model to simulate karst sinkholes: A case study in Southwest China. *Frontiers in Environmental Science* 10, 950098, doi: 10.3389/fenvs.2022.950098.

Cite as: Ścigała, R., Szafulera, K., Jendryś, M. (2023) Assessment of sinkhole hazard in the post-mining area using the ERT method and numerical modeling. *Scientific Journals of the Maritime University of Szczecin, Zeszyty Naukowe Akademii Morskiej w Szczecinie* 75 (147), 20–34.